

1 This is a post-peer-review, pre-copyedit version of an article published in the *Annals of*
2 *Geophysics*. The final authenticated version is available online at:

3 <https://doi.org/10.4401/ag-8019>

4
5 **CHARACTERIZATION OF HISTORICAL MASONRY MORTAR FROM SITES**
6 **DAMAGED DURING THE CENTRAL ITALY 2016-2017 SEISMIC SEQUENCE: THE CASE**
7 **STUDY OF ARQUATA DEL TRONTO**

8 **MORTARS FROM ANCIENT TOWNS IN CENTRAL ITALY** (40 characters)

9 Daniele MIRABILE GATTIA¹, Graziella ROSELLI², Omar ALSHAWA³, Paolo CINAGLIA⁴, Giuseppe DI
10 GIROLAMI⁴, Cristina FRANCOLA³, Franca PERSIA¹, Enrica PETRUCCI⁵, Roberto PILONI², Fabrizio
11 SCOGNAMIGLIO⁴, Luigi SORRENTINO³, Silvia ZAMPONI², Domenico LIBERATORE³

12
13 ¹ *Department of Sustainability SSPT - ENEA - CR Casaccia, Via Anguillarese 301, 00123 Rome, Italy;*

14 daniele.mirabile@enea.it, franca.persia@enea.it

15 ² *School of Science and Technology, Chemistry Division, University of Camerino, Via S. Agostino 1, 62032 Camerino,*
16 *Italy;*

17 graziella.roselli@unicam.it, roberto.piloni@unicam.it, silvia.zamponi@unicam.it

18 ³ *Department of Structural and Geotechnical Engineering, "Sapienza" University of Rome, Rome, Italy;*

19 domenico.liberatore@uniroma1.it, omar.alshawa@uniroma1.it, francola.cristina@gmail.com,

20 luigi.sorrentino@uniroma1.it

21 ⁴ *School of Science and Technology, Technologies and Diagnostics for Conservation and Restoration Laboratory,*
22 *University of Camerino, Via Pacifici Mazzoni 2, 63100 Ascoli Piceno, Italy;*

23 paolo.cinaglia@unicam.it, giuseppe.digirolami@unicam.it, fabrizio.scognamiglio@unicam.it

24 ⁵ *School of Architecture and Design, University of Camerino, 63100 Ascoli Piceno, Italy;*

25 enrica.petrucci@unicam.it

26
27 **Abstract**

28 Mortar quality is a fundamental parameter to take into account when studying the structural behavior of
29 masonry, especially under seismic actions. Separation between the leaves of rubble masonry can occur, inducing
30 the partial or total collapse of the construction. A good quality mortar is essential to delay/prevent the separation
31 of leaves, but often, especially in ancient building with a cultural value, mortars have low binder capabilities.

32 The paper presents an experimental investigation on mortar specimens taken from buildings of a little
33 municipality in Marche region, Arquata del Tronto, heavily damaged by recent earthquakes in Central Italy
34 (2016-2017). Both diagnostic techniques as X-Ray diffraction, Fourier-Transform infrared spectroscopy and
35 calcimetry, and mechanical test as compression tests were carried out in order to correlate the obtained values
36 with the performance of the original masonry.

37
38 **1. Introduction**

39 The damage caused by the 2016-2017 Central Italy earthquakes to architectural heritage in the municipalities of
40 Marche region were very high. In Arquata del Tronto, a small town in the province of Ascoli Piceno, the
41 earthquakes caused collapses and damage of churches, monuments and cultural heritage, as well of buildings in
42 small neighboring villages.

43 From the macro-seismic point of view the municipality of Arquata, as well as the other localities in the same
 44 area, was historically subjected to significant earthquakes interspersed with periods of seismic inactivity: as
 45 shown in table 1, in which only recent seismic events with a level of damage greater than or equal to the VI MCS
 46 are reported, it is possible to note that a long period of calm goes from the shock on May 12th, 1730 (VII-VIII
 47 MCS) to that on July 4th, 1916 (VII MCS).

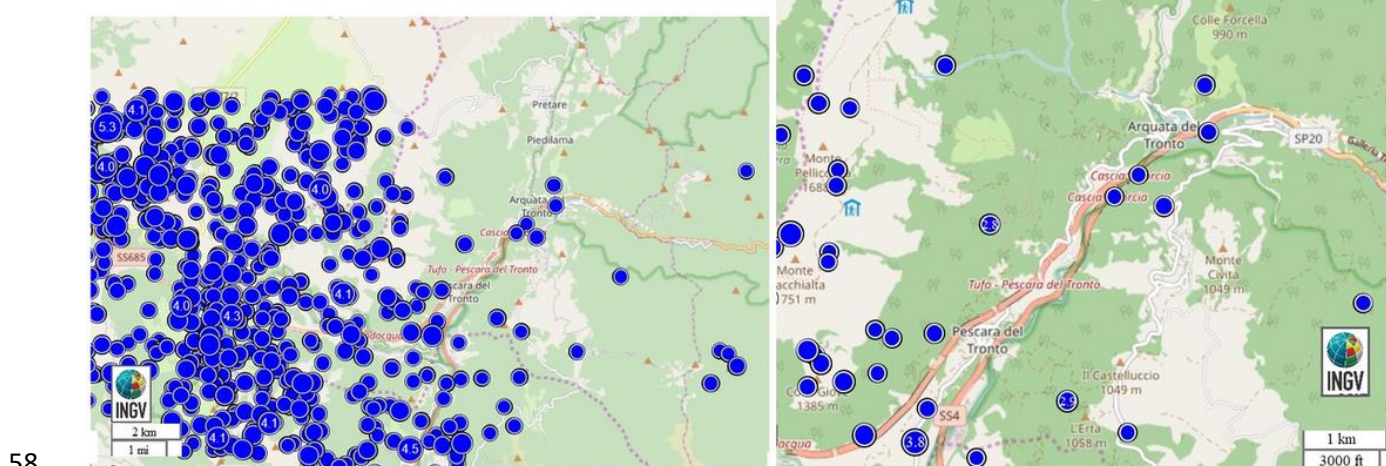
48
49

50 **Table 1. Recent earthquakes in Central Italy with a level of damage greater than or equal to the VI MCS [Locati et al., 2016;**
 51 **Albini et al., 2016]**

MCS \geq VI	Date	Epicenter
IX	January 14 th , 1703	Valnerina
VII-VIII	May 12 th , 1730	Valnerina
VII	July 4 th , 1916	Sibylline Mountains
VI	April 7 th , 1930	Sibylline Mountains
VI	December 19 th , 1941	Sibylline Mountains
VI	January 29 th , 1943	Sibylline Mountains
VI	October 3 rd , 1943	Area of Ascoli Piceno
VI-VII	September 5 th , 1950	Gran Sasso d'Italia
VI-VII	November 26 th , 1972	Southern Marche
VI	September 19 th , 1979	Valnerina
VIII-IX	August 24 th , 2016	Area of Amatrice

52

53 The shock on August 24th, 2016 caused damage associated to the IX degree of the MCS. Although damage was
 54 more severe in the surrounding villages, only a few buildings collapsed in the main square, whereas all the others
 55 were damaged. With the event on October 30th of the same year (fig. 1) the scenario changed radically: Arquata
 56 was completely destroyed. The Italian Army and the firefighters started the debris removal and the realization of
 57 a *tabula rasa* in all the Arquata promontory.



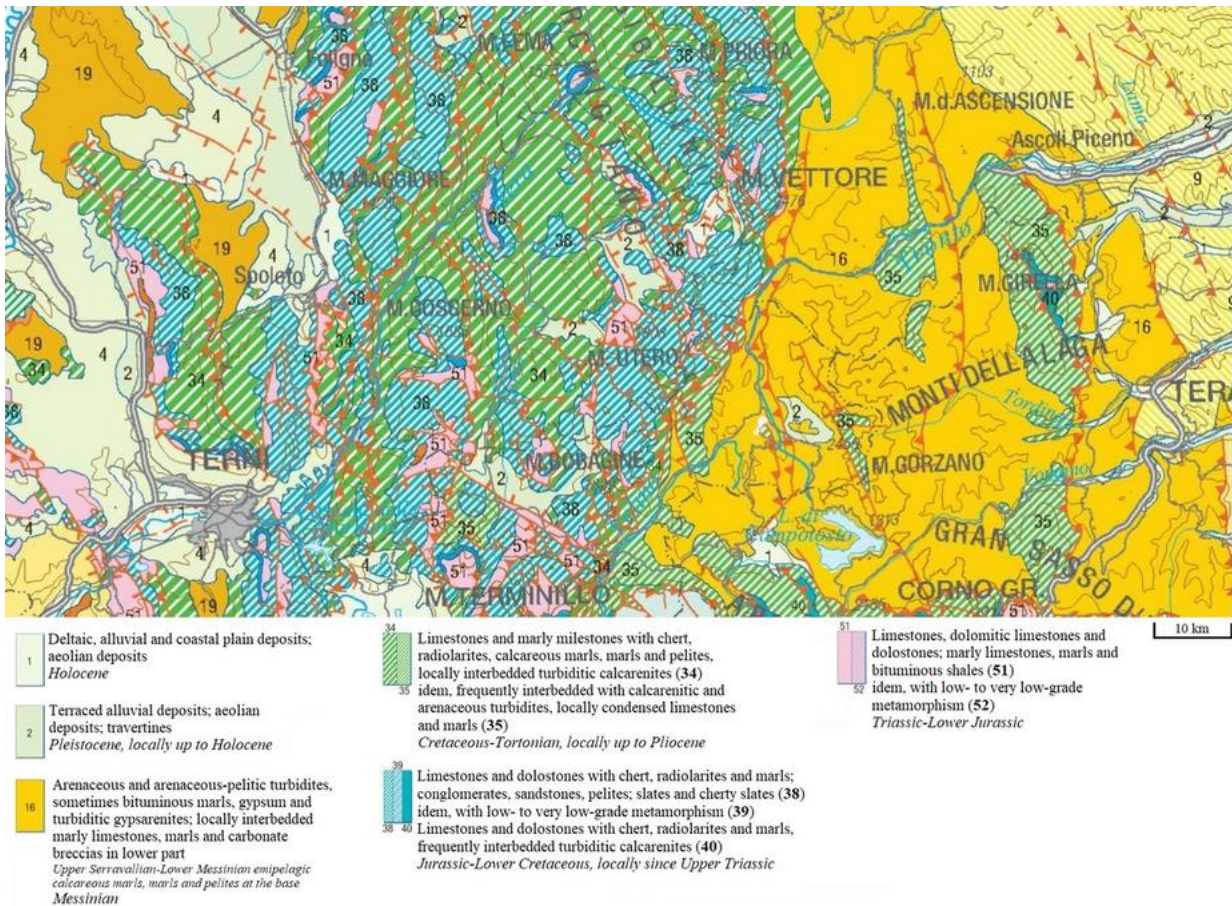
58

59 **Fig. 1. Earthquakes registered, between 2016 and 2017, in the area surrounding Arquata del Tronto with magnitude higher than**
 60 **2.5. The events of magnitude from 3.8 to 4.1 on October 30th, 2016 are shown. Left, larger scale; right, smaller scale (source:**
 61 **INGV¹)**

¹ Data and results published on this website by Istituto Nazionale di Geofisica e Vulcanologia (<http://www.ingv.it/>) are licensed under a Creative Commons Attribution 4.0 International License (<http://creativecommons.org/licenses/by/4.0/>). ISIDe Working Group at National Earthquake Center (<http://cnt.rm.ingv.it/>) benefited from funding provided by the Italian Presidenza del Consiglio dei Ministri, Dipartimento della Protezione Civile.

62
63
64
65
66
67
68
69
70

The 2016 seismic sequence affected a portion of the Apennines characterized by the outcrop of turbiditic sandstones (Laga Flysch, Messinian), limestones and pelagic marly limestones of the Umbro-Marchigiana series (Mesozoic) (fig. 2). These lithologies are the most common construction material of the buildings erected until the sixties of the last century, as well as of all the monumental buildings as churches, castles, towers and convents. An in-depth study on the architectural heritage in the territory of Arquata del Tronto shows that the masonry structures follow a building practice which changed during time, entailing substantial variations of their load bearing capacity. Local materials were used for masonry, with differences between the zones north and south of river Tronto.



71
72
73

Fig. 2. Geological map (1:1000000) relative to Arquata del Tronto and surroundings (source: ISPRA²)

74 The southern zone is characterized by sandstone mixed with river pebbles, with rare brick units, whereas the
75 northern zone by limestones added to masonry. The masonry fabric consists of irregularly rough-hewed units
76 and chips of natural materials. The mortar is poor of lime and particularly crumbly. Irregularities are
77 compensated by plentiful mortar. A limited compliance of the horizontal orientation can be observed.
78 Sometimes the horizontality of courses is provided by the insertion of brick wedges. The offset of head joints is
79 nearly absent. Several buildings are in complete abandonment since decades, and some of them were near
80 collapse already before the earthquake. At the same time there are inhabited buildings in normal maintenance
81 conditions, where relatively recent interventions were carried out, with ring beams and roofs in reinforced
82 concrete, in some cases with smooth rebars, not linked each other and without hoops. As already observed after

² www.isprambiente.gov.it.

83 the 1997 Umbria-Marche earthquake and the 2009 L'Aquila earthquake, these intervention, without a proper
84 consolidation of the vertical structure, usually entailed widespread collapses.

85 Although it is aware that the seismic effects on structures depend on a plurality of factors, like the energy
86 released by the earthquake, the geological characteristics of the site, the type of foundation, the original
87 materials and techniques, but also the state of conservation of the buildings and possible maintenance actions
88 occurred during the time [Guidoboni and Ferrari, 2009], developing a methodology to define mortar quality
89 would be very useful to interpret the mutual relationship and the correlation between earthquake and damage.
90 With this aim, a sampling campaign in Arquata and its neighboring villages was carried out, in order to
91 chemically and mechanically characterize the mortar and correlate the obtained values with the performance of
92 the original masonry.
93

94 2. Experimental setup or method

95 Twenty-four mortar samples have been collected, under the supervision of firefighters, from historical and
96 monumental buildings located in different settlements within the municipality of Arquata del Tronto (table 2 and
97 fig. 3). Sampling has been performed with care considering only bedding mortars from collapsed or partially
98 collapsed buildings.

99 **Table 2. Mortar samples from settlements within the municipality of Arquata del Tronto**

Settlement	Sample ID
Arquata del Tronto	1
	2
	3
	4
	5
Borgo	6
	7
	8
	9
	10
Camartina	11
	12
	13
Faete	14
	15
	16
	17
Pretare	18
	19
	20
	21
Trisungo	22
	23
	24

100

101 During sampling, for each mortar specimen a record card has been filled with: date, location, type of building,
102 point of sampling, sample quantity (estimated).



103
104 **Fig. 3. Mortar sampling campaign in Pretare - St. Rocco Church (Arquata del Tronto)**

105 Firstly, an inspection of the samples collected has been carried out, in order to remove possible impurities and to
106 exclude samples that presented effects of external agents. The inspection has been made in laboratory, both with
107 naked eye and a stereomicroscope Olympus SZX12 with digital image acquisition.

108 Possible contaminations could be due to the collapse of the structure itself, causing contact with other materials,
109 or from subsequent contact with external agents (natural or anthropic). For instance, some mortar samples have
110 been excluded from the analysis as they presented the formation of plants probably due to exposure to a humid
111 environment.

112 Then, to evaluate grain size distribution the samples have been firstly roughly cracked in smaller pieces and
113 successively they have been sieved. Different mechanical treatments have been performed in dry conditions and
114 the material passing through the sieve has been weighted and recovered [Groot et al., 1996]. Particle-size
115 analysis was carried out using the following sieves: 2.000, 1.000, 0.500, 0.250, 0.106, 0.063 mm.

116 The samples were analysed by X-Ray diffraction in order to evaluate the type of binder and aggregate. This
117 technique allows identifying crystalline phases, while the presence of amorphous phases generates broad halos
118 in the pattern.

119 A SmartLab Rigaku powder diffractometer, equipped with Cu $\kappa\alpha$ radiation source and a graphite
120 monochromator in the diffracted beam, operated at 40kV and 30 mA, has been used. X-Ray diffraction powder
121 patterns have been acquired within the angular range 2-90 2θ at a step size of 0.04 and 12 seconds per step. In
122 order to enhance the binder fraction the disaggregated mortars have been sieved at 63 μm and the powder
123 obtained has been successively grinded in order to further reduce particles dimensions [Carrara and Persia,
124 2001; Cardinale et al., 2002]. Some samples have been analysed also after removal of larger inert coarser
125 granule and refining the powders using an agate mortar [Chiari et al., 1993].

126 Analysis by Fourier-Transform Infrared Spectroscopy (FT-IR) was carried out on mortar samples ground in a
127 agate mortar and then passed completely through a 125 μm sieve. A Perkin Elmer Spectrum 100 was used in
128 ATR mode (Total Reflected Reflectance). For each sample two acquisitions were performed.

129 Calcimetry has been performed, using the gas-volumetric Dietrich-Fruhling method. The sample was ground
130 manually with an agate mortar until it was completely passed through a 63 μm sieve, then dried into a

131 thermobalance at 60 °C up to constant mass. The sample was treated with a reagent based on hydrochloric acid,
132 which decomposes the carbonates present by CO₂ development, as regulated by UNI 11140: 2004. This
133 technique allowed to evaluate with greater precision, compared to the analysis in FT-IR spectroscopy ATR, the
134 quantity of carbonates present in the samples (uncertainty: ± 0.1%).

135 Soluble salt content was estimated by conductometric measurements. From the conductivity value of the
136 solutions, the formula indicated in the DIMOS document, part II module 3, ICR, 1978 was applied, estimating
137 the percentage of soluble salts present in the samples. Analysis of soluble salts (UNI 11087: 2003) was carried
138 out as following: the sample was dried in an oven at 60 °C for about 24 h, then ground manually within an agate
139 mortar until it was completely passed through a 125 µm sieve. The samples were weighed (95 mg up to 105 mg)
140 and treated into a thermobalance at a temperature of 60 °C up to constant mass. 100 ml of bi-distilled H₂O,
141 whose conductivity was previously measured, were added to the sample and placed in a flat-bottomed glass
142 container. The container was hermetically sealed to prevent evaporation and slowly stirred for 2h; then residuals
143 were left to deposit for about 30 min; finally, conductivity was measured with a XS Multiparameter, model PC
144 70 (resolution: 0.1 µS). The obtained suspension was then filtered (black band filter) and the solution was used
145 for the measurements of the single ionic species by ionic chromatography.

146 Concentration of anions contained in mortar under study has been measured with a Metrohm Ion
147 Chromatograph 761 Compact with chemical integrated Metrohm suppressor module (MSM) and METROSEP
148 A Supp. 5 150/4.0 separation column. Injection volume was typically 1.5 ml and the loop volume was 20 µl.
149 Sartorius 0.45 µm RC-Membrane PP-Housing filters were used to remove particles. Three repetition for each
150 analysis were performed. The method of calibration curve with increasing concentrations of standards has been
151 used to calculate the concentration of anions.

152 Prismatic specimens were obtained from field samples, the edges were measured, the top and bottom faces were
153 covered with plaster and a compression test was performed. The tests were performed under displacement
154 control at a speed of 0.54 mm/min. Strain was calculated dividing the relative displacement between the load cell
155 and the base plate by the initial distance. The measurement was not taken directly on the sample because of the
156 large size of the aggregate. For each sample, the stress-strain curve was elaborated. The normalized compressive
157 strength f_m was determined multiplying the nominal strength f by the shape factor δ :
158

$$f_m = \delta f \quad (1)$$

159 The shape factor δ , which accounts for the sample geometry, was calculated according to [BS EN 772-1:2011 +
160 A1:2015, 2015].

161 Since no standard is available for the determination of the modulus of elasticity of masonry mortar, that
162 recommended for concrete was used [ASTM C 469 – 02, 2002]. Thus, the modulus of elasticity E is given by:
163
164

$$E = \frac{S_2 - S_1}{\varepsilon_2 - \varepsilon_1} \quad (2)$$

165 where:

166 $S_2 = 40\%$ of the nominal compressive strength f ;

167 $S_1 =$ stress corresponding to strain ε_1 ;

168 $\varepsilon_2 =$ strain corresponding to stress S_2 ;

170 $\varepsilon_1 = 0.00005$.

171

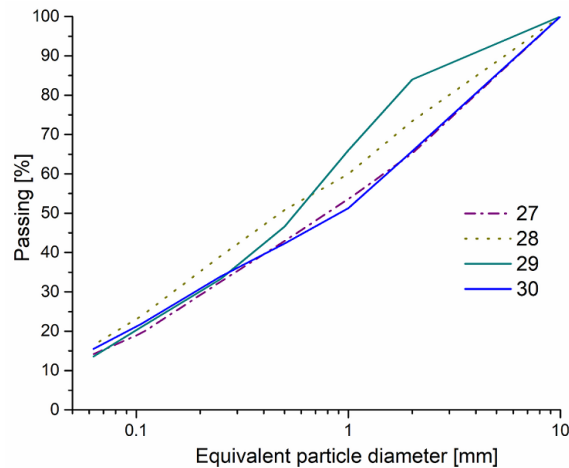
172 As for the measurement of strain, the beginning of the test was identified when the load was monotonically
173 increasing under a prescribed monotonically increasing displacement.

174

175 3. Results and discussion

176 3.1 Sieving process and grain size distribution

177 Particle-size distribution highlighted the preponderance of a fine fraction in mortar samples, especially those
178 from Pretare, as shown in fig. 4.



179

180

181

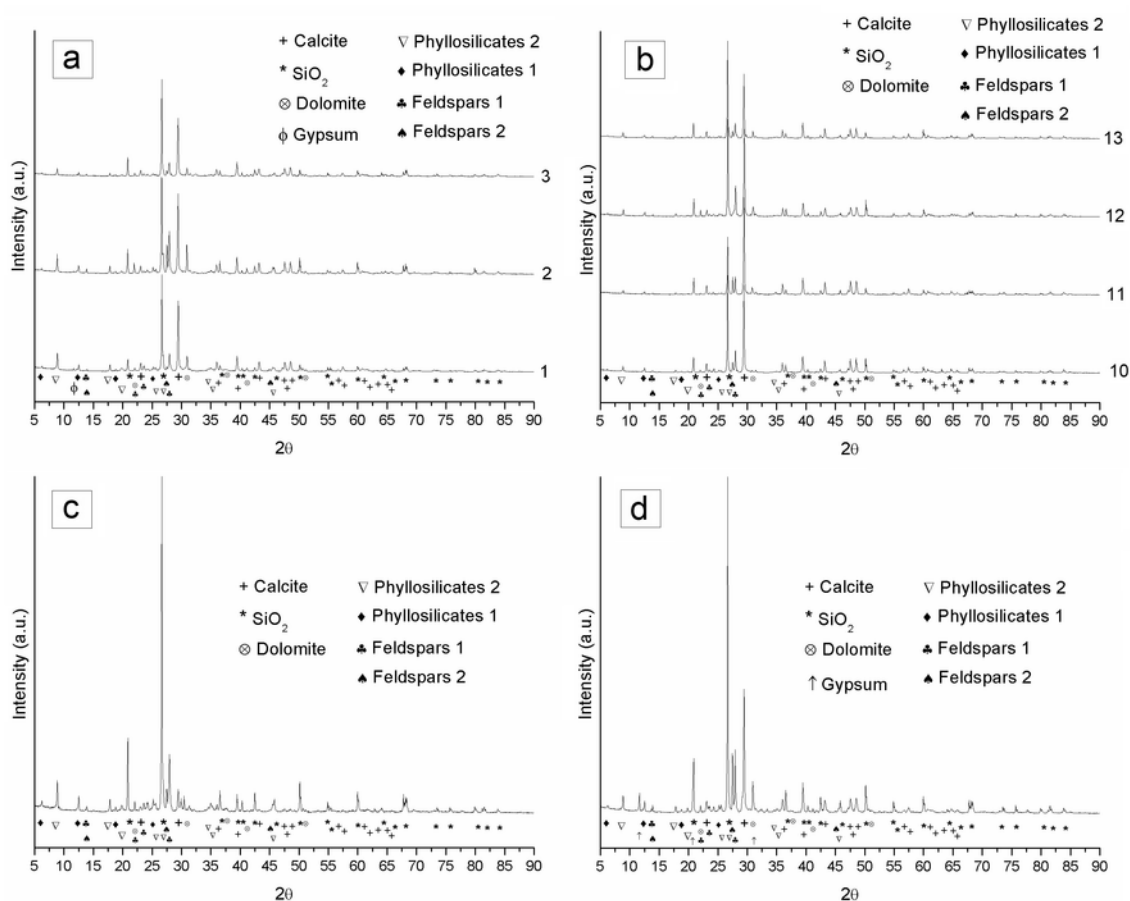
Fig. 4. Particle-size analysis

182 In some cases the finer fractions, smaller than 0.5 mm, constitute more than 40% of the entire aggregates.

183

184 3.2 X-Ray diffraction

185 In fig. 5 XRD patterns of mortars from Arquata del Tronto (1, 2, 3), Camartina (10, 11, 12, 13), Faete (14) and
186 Trisungo (24) are shown. The samples from Arquata presented principally quartz, calcite, phyllosilicates,
187 feldspars and dolomite, in particular in sample 2 and some traces of gypsum. Same phases were identified in the
188 samples from Camartina, even if only traces of dolomite were present while gypsum was absent. Sample 11
189 from Camartina presented higher quantity of calcite with respect to the other samples. Material sampled in Faete
190 revealed small quantity of calcite, being quartz the most abundant phase. The sample from Trisungo presented
191 similar phases respect to those from Arquata but also gypsum and lower concentrations of calcite. It has to be
192 noted that no crystalline phases related to hydraulic binders have been detected in all the samples investigated.
193 X-Ray diffraction data could give important indication about binder and aggregates even if it should be
194 considered that the detection limit of the technique is about 1 wt%.



195

196
197

Fig. 5. XRD patterns of samples from a) Arquata del Tronto (1, 2, 3), b) Camartina (10, 11, 12, 13), c) Faete (14) and d) Trisungo (24)

198
199
200

Moreover, eventual non crystalline phases deriving from carbonation and hardening, as amorphous calcium silica gel (C-S-H), deriving from hydration of cement, could not be detected. In some samples large quantities of calcite have been detected being probably related in part to aggregate fraction [Chiari et al., 1992].

201
202
203
204

The dolomite recognized in the samples was probably used as aggregate, because peaks related to hydromagnesite and hydrated magnesium carbonate hydroxide have not been detected in the XRD patterns. The presence of hydromagnesite deriving from mortars with binders deriving from dolomite as precursor is still controversial [Montoya et al., 2003].

205
206

As just stated above and referring to the geological map, the analysis of the materials sampled are in agreement with the hypothesis that the construction materials were extracted around these small towns.

207
208
209

3.3 Fourier-Transform Infrared Spectroscopy, calcimetry, soluble salt analysis and dosage of anionic species

210
211
212

FT-IR analysis allowed to gain an overview of the composition of the mortars [Gulmini et al., 2015] and, relatively to carbonates, silicates and sulphates, the intensity of their stretching signals have been used to obtain a semi-quantitative evaluation (table 3).

213
214

Table 3. FT-IR results and percentage of carbonates in mortars analyzed from settlements within the municipality of Arquata del Tronto. The intensity of the stretching signals of carbonates, silicates and sulphates is indicated by the number of ‘x’

Settlement	Sample ID	FT-IR			Calcimetry
		CO ₃ ²⁻	SiO ₄ ⁴⁻	SO ₄ ²⁻	[% of carbonates]
Arquata del Tronto	1	xx*	xxx		26.5
	2	xx*	xx	(x)	21.1
	3	x	xx		16.5
	4	xxx			95.6
	5	xxx	xx		52.6
Borgo	6	xxx*	xx		51.9
	7	xxx	xxx		35.4
	8	xxx	xx**		32.9
	9	xxx	x**		62.2
	10	xxx	xx		50.0
Camartina	11	xxx	xx		50.9
	12	xxx	xx		44.5
	13	xxx	xxx		36.9
Faete	14	x	xxx		16.6
	15	xxx*	x		76.4
	16	xxx*	x		54.4
	17	xxx*	(x)		30.5
Pretare	18	xxx*	x		39.3
	19	xxx*	x		95.1
	20	xxx	x		76.7
	21	xxx	x		73.5
	22	xxx*	(x)		32.7
Trisungo	23	x	xx**		17.6
	24	x*	xxx	xx	11.0

215
216
217
218

* presence of dolomite, in addition to calcite

** presence of phyllosilicates, in addition to quartz

219 The most part of mortars collected show intense signals of carbonates, as confirmed by calcimetry: eighteen
220 samples have a percentage of carbonates higher than 30%; eleven of them have a percentage well above 50%
221 (table 3), indicating that the aggregate is partially made by carbonates. According to XRD results, in some
222 specimens FT-IR analysis highlighted the presence of dolomite.

223 In regard to the soluble salt analysis by conductimetry, the mortars are characterized by percentages between 2
224 and 10%, with the exception of sample 24 (table 4).

Table 4. Percentage of Soluble Salts (SS) and concentration of anionic species (average value of three measurements and associated standard deviation) in mortars analyzed from settlements within the municipality of Arquata del Tronto

Settlement	Sample ID	Conductivity	SS	F ⁻	Cl ⁻	NO ₃ ⁻	PO ₄ ³⁻	SO ₄ ²⁻
		[μS]	[%]			[ppm]		
Arquata del Tronto	1	62.1	4.1	-	2.11±0.12	2.64±0.36	-	2.18±0.21
	2	105.8	7.1	-	5.84±0.49	9.63±0.19	-	9.78±0.60
	3	62.5	4.2	-	1.07±0.07	-	-	1.72±0.25
	4	45.3	2.9	-	0.43±0.02	0.65±0.05	-	>0.5
	5	92.1	5.9	-	0.98±0.04	19.17±0.17	-	1.00±0.04
Borgo	6	54.3	3.4	-	0.57±0.11	0.45±0.05	-	0.90±0.17
	7	40.2	2.4	-	0.38±0.03	-	-	>0.5
	8	56.3	3.6	-	0.83±0.01	0.74±0.05	-	-
	9	82.5	5.2	-	1.08±0.16	13.56±1.22	-	-
Camartina	10	44.8	3.0	-	<0.25	-	-	<0.25
	11	52.0	3.4	-	<0.25	-	-	<0.25

	12	49.5	3.2	-	1.50±0.06	3.57±0.34	-	<0.25
	13	57.4	3.8	-	0.54±0.11	0.76±0.05	-	<0.25
Faete	14	67.5	4.4	-	2.43±0.31	3.10±0.56	-	-
	15	78.9	5.0	-	0.50±0.03	0.45±0.05	-	>0.5
	16	65.2	4.0	-	1.04±0.17	1.50±0.29	-	8.84±1.05
	17	125.4	8.3	-	0.33±0.01	0.30±0.20	-	0.51±0.13
Pretare	18	45.5	2.8	-	0.52±0.01	-	-	0.67±0.05
	19	61.1	4.1	-	0.50±0.07	1.15±0.20	-	0.92±0.10
	20	158.3	10.0	-	2.57±0.01	13.14±1.5	-	0.65±0.05
	21							
	22	66.2	4.0	-	0.59±0.09	0.24±0.05	-	1.07±0.12
Trisungo	23	93.5	5.9	-	5.00±0.05	13.70±1.79	-	3.87±0.64
	24	177.9	11.9	-	2.07±0.05	3.39±0.37	-	61.17±0.41

227

228 Concerning the concentration of the various anionic species (table 4), the following considerations can be made:

- 229 - the sulphates were present in low quantities, below 3 ppm (except for samples 2, 16, 23 and 24);
 230 - the presence of chlorides in the samples is negligible: only two samples exceed 3 ppm (2 and 23);
 231 - regarding nitrates there is a very heterogeneous situation, with values between 0,24 and 19,17 ppm;
 232 - presence of fluorides and phosphates was not detected.

233

234 3.4 Compression tests

235 Some samples, although containing calcite, presented poor compactness and they could be easily fragmented.
 236 Mechanical tests have been performed on the samples that presented the highest compactness and in particular
 237 those that could be cut to a shape suitable for tests without fragmentation. Two specimens were obtained from
 238 sample 17, collected at Pretare. The prismatic samples, tested in compression, are shown in fig. 6.



239

240

241

242

243

244

Fig. 6. Cubic samples obtained from sample 17: left, sample 17.1; right, sample 17.2

Their dimensions are reported in table 5, along with the corresponding shape factor.

245
246

Table 5. Characteristics of the samples tested in compression

Sample	Weight (g)	Length (mm)	Width (mm)	Cross-section area (mm ²)	Height (mm)	Density (kg/m ³)	Shape factor (-)
17.1	154	49	54	2660	45	1284	0.821
17.2	149	50	55	2739	44	1235	0.816

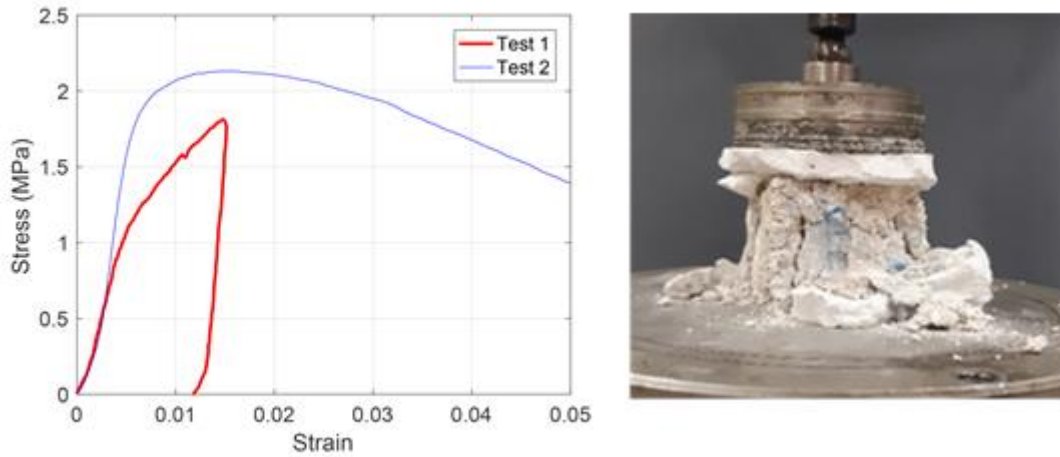
247

248 It is mandatory to emphasise that these specimens were obtained from a sample having an above-average
249 compactness compared to those collected in the municipality.

250

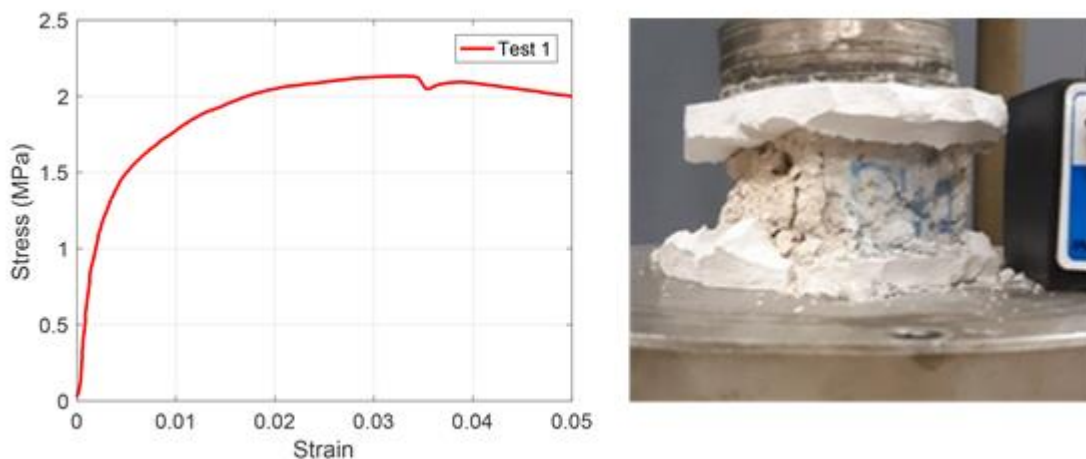
251 For sample 17.1, a first test was performed that did not reach failure, and a second test until failure. For sample
252 17.2, failure was reached at the first test. For each sample, the stress-strain curve is reported in figs. 7-8, along
253 with a picture of the sample at the end of the test.

254



255
256
257

Fig. 7. Sample 17.1: left, stress-strain curve; right, sample at the end of the test



258
259
260
261

Fig. 8. Sample 17.2: left, stress-strain curve; right, sample at the end of the test

262 The normalized compressive strength f_m was calculated according to Eq. (1). The results are reported in table 6,
 263 where, for the test that did not reach failure:
 264 F_{max} = maximum load;
 265 σ_{max} = maximum stress;
 266 ε_{max} = strain at maximum stress;
 267 ε_r = residual strain;
 268 and, for the tests that reached failure:
 269 F_u = ultimate load;
 270 f = nominal strength;
 271 ε_f = strain corresponding to ultimate load.

272
 273 **Table 6. Results of compression tests**

Sample	Failure	F_{max} (kN)	σ_{max} (MPa)	ε_{max}	ε_r	F_u (kN)	F (MPa)	f_m (MPa)	ε_f
17.1	No	5.0	1.88	0.015	0.012	-	-	-	-
	Yes	-	-	-	-	5.8	2.18	1.79	0.015
17.2	Yes	-	-	-	-	6.0	2.19	1.79	0.035

274
 275 The two samples highlight an almost perfect match in terms of strength, but a significant difference in terms of
 276 strain at ultimate load. Such difference could be ascribed to sample scatter, to disturbance introduced during
 277 sample preparation or, more likely, to the fact that sample 17.1 underwent a first test before the failure one.
 278 The strength value can be compared with the 60 values collected from literature in [Liberatore et al., 2014] for
 279 clay brickwork: there are six samples with a smaller strength (the smallest being 0.28 MPa). If the 42 sample of
 280 tuffwork in [Marotta et al., 2016] are considered, Arquata's samples are larger of just four values (minimum
 281 value 0.55 MPa). Additionally, it is worth emphasising that the current Italian building code [DMIT, 2018]
 282 prescribes a minimum strength of 2.5 MPa for ordinary loads (Sect. 11.10.2), and 5.0 MPa under earthquake
 283 loads (Sect. 7.8.1). Instrumental error of the load cell is declared by the manufacturer as $\pm 0.5\%$, and the same
 284 error can be assumed for strength estimation.
 285 Additionally, it is useful to emphasise that mortar deformation capacities are seldom reported, hence, enhancing
 286 the importance of data reported herein that is necessary for non-linear micromechanical modelling [Zucchini
 287 and Lourenco, 2007]. Instrumental error of the displacement transducer is $\pm 1.0\%$, and the same error can be
 288 assumed for deformation estimation.
 289
 290 Finally, modulus of elasticity of masonry mortar, reported in table 7, presents a scatter greater than that of
 291 strength. Sample 17.1 has a modulus of elasticity nearly constant during the two tests. Observed values are very
 292 low compared to the seven in [Liberatore et al., 2014] all larger than 1 GPa. The worst combination of
 293 instrumental error in load cell and displacement transducer leads to a Young's modulus measurement
 294 uncertainty of $\pm 0.6\%$.

295 **Table 7. Modulus of elasticity**

Sample	Failure	S_2 (MPa)	S_1 (MPa)	ε_2 (-)	E (MPa)
17.1	No	0.85	0.01	0.0038	223
	Yes	0.85	0.01	0.0033	258
17.2	Yes	0.85	0.04	0.0014	615

296

297 **Conclusions**

298 During 2016 and 2017 a dramatic sequence of seismic events heavily damaged small towns in the Centre of Italy
299 in regions as Lazio, Abruzzo, Marche and Umbria, causing a large number of victims.

300 In this work the bedding mortars of some masonry partially or completely collapsed during earthquakes have
301 been sampled in the surroundings of Arquata del Tronto and analyzed by different techniques.

302 X-Ray diffraction analysis revealed the use of lime mortars with the presence mainly of quartz and calcite and
303 the presence of feldspars and phyllosilicates. In some cases dolomite has been identified. Some samples also
304 evidenced the absence of the binder or its presence in traces. FTIR and Calcimetry confirmed the presence of
305 carbonates and silicates and that of dolomite in some specimens, while other measurements revealed the
306 presence of low concentrations of soluble salts.

307 Several samples presented poor mechanical characteristics and could be easily fragmented. Compression tests
308 have been performed on two samples that showed higher cohesion and could be worked without fragmentation.

309 The tests showed that the mortar, of presumed lime type from calcareous and dolomitic rocks, has poor
310 mechanical behavior, with normalized compressive strength lower than 1.8 MPa, i.e. at the lower bound of the
311 values reported in the literature, and significantly lower than the minimum strength prescribed by the code for
312 new constructions in seismic prone areas (5 MPa). Similar results were found for the modulus of elasticity. This
313 work evidences, through a multidisciplinary approach, some highlights on the bedding mortars used in these
314 historical sites. The results of the analysis reported in this paper could be useful as support for future research,
315 supplying information for establishing priorities of intervention for repairing and consolidation and also for
316 reconstruction activities which would take into account construction materials of this ancient masonries. In the
317 future a campaign of measurements could be carried out in order to design a sort of vulnerability map of
318 masonries as aid for lawmakers, municipalities and experts.

319

320 **References**

321 - Albinì, P., L. Arcoraci, M. Berardi, F. Bernardini, C. Bignami, B. Brizuela, R. Camassi, V. Castelli, C.
322 Castellano, S. D'Amico, V. D'Amico, S. Del Mese, E. Ercolani, A. Fodarella, L. Graziani, M. Locati, I.
323 Leschiutta, A. Maramai, V. Pessina, A. Piscini, A. Rossi, A. Rovida and M. Sbarra (2016). QUEST - Rilievo
324 macrosismico in EMS98 per il terremoto di Amatrice del 24 agosto 2016 – Report finale, www.questingv.it.

325 - ASTM C 469 - 02 (2002). Standard Test Method for Static Modulus of Elasticity and Poisson's Ratio of
326 Concrete in Compression, ASTM International, West Conshohocken, PA, 2014, www.astm.org, DOI:
327 10.1520/C0469_C0469M-14.

328 - BS EN 772-1:2011 + A1:2015 (2015). Methods of test for masonry units. Determination of compressive
329 strength.

330 - Cardinale, V., F. Persia, L. Campanella, F. Cardellini and S. Omarini (2002). Storia costruttiva del complesso
331 monastico di San Vincenzo al Volturno attraverso la determinazione di differenze composizionali nelle malte.
332 Risultati preliminari, Atti del 2° Congresso Nazionale AIAR, Bologna 29 gennaio-1 febbraio 2002, 505-513,
333 ISBN 88-555-2688.

334 - Carrara, C. and F. Persia (2001). Indagini mineralogiche-petrografiche e di diffrazione dei raggi X sulle
335 incrostazioni calcaree e sulle malte in Gli acquedotti Claudio e Aniene Nuovo nell'area della Banca d'Italia in
336 Via Tuscolana, Ed Istituto Poligrafico e Zecca dello Stato, 193-197.

337 - Chiari, G., M.L. Santarelli and G. Torraca (1992). Caratterizzazione delle malte antiche mediante l'analisi di
338 campioni non frazionati, anno II, n. 3.

339 - Chiari, G., M.L. Santarelli and G. Torraca (1993). Caratterizzazione delle malte antiche mediante l'analisi di
340 campioni non frazionati, *Materiali e Strutture*, 2, 111-137.

- 341 - DMIT (2018). Decreto del Ministro delle Infrastrutture e dei Trasporti 17 gennaio 2018. Aggiornamento delle
342 “Norme tecniche per le costruzioni”. Gazzetta Ufficiale della Repubblica Italiana, n. 42 del 20 febbraio 2018,
343 Supplemento Ordinario n. 8.
- 344 - Groot, C., G. Ashall and J. Hughes (1996). Characterization of Old Mortars with Respect to their Repair, Final
345 Report of RILEM TC 167-COM.
- 346 - Guidoboni, E. and G. Ferrari (2009). Historical variables of seismic effects: economic levels, demographic
347 scales and building techniques, *Annals of Geophysics*, 43 (4), 687-705.
- 348 - Gulmini, M., G. Roselli, F. Scognamiglio and G. Vaggelli (2015). Composition and microstructure of maiolica
349 from the museum of ceramics in Ascoli Piceno (Italy): evidences by electron microscopy and microanalysis,
350 *Applied Physics A*, 120 (4), 1643-1652.
- 351 - Liberatore, D., A. Marotta and L. Sorrentino (2014). Estimation of clay-brick unreinforced masonry
352 compressive strength based on mortar and unit mechanical parameters, 9th International Masonry Conference,
353 Guimaraes, Portugal, 5-7 July, paper 1400, 12 pp.
- 354 - Locati, M., R. Camassi, A. Rovida, E. Ercolani, F. Bernardini, V. Castelli, C.H. Caracciolo, A. Tertulliani, A.
355 Rossi, R. Azzaro, S. D’Amico, S. Conte and E. Rocchetti (2016). DBMI15, the 2015 version of the Italian
356 Macroseismic Database, Istituto Nazionale di Geofisica e Vulcanologia, DOI:
357 <http://doi.org/10.6092/INGV.IT-DBMI15>.
- 358 - Marotta, A., D. Liberatore and L. Sorrentino (2016). Estimation of unreinforced tuff masonry compressive
359 strength based on mortar and unit mechanical parameters, *Brick and Block Masonry: Trends, Innovations and
360 Challenges - Proceedings of the 16th International Brick and Block Masonry Conference, IBMAC 2016,*
361 *1715-1722.*
- 362 - Montoya, C., J. Lanás, M. Arandigoyen, I. Navarro, P.J. García Casado and J.I. Alvarez (2003). Study of
363 ancient dolomitic mortars of the church of Santa María de Zamarce in Navarra (Spain): Comparison with
364 simulated standards, *Thermochimica Acta*, 398(1), 107-122.
- 365 - Zucchini, A. and P.B. Lourenço (2007). Mechanics of masonry in compression: Results from a
366 homogenisation approach, *Computers and Structures*, 85, 193–204.